PHYM004 Project 2: Smoothed Particle Hydrodynamics

Jay Malhotra

March 24, 2022

1 Introduction

Smoothed-particle hydrodynamics (SPH) is an approach to the numerical simulation of fluid dynamics. Notable characteristics of this method include the fact that it is mesh-free, and that it is derived using Lagrangian mechanics, which gives it good conservation properties.

This report presents a one-dimensional SPH code which is capable of reproducing some basic analytical results. It features artificial viscosity calculation and a method for varying the smoothing length on a per-particle basis using a root-finding algorithm.

1.1 Equations of motion

Price (2012) provides a full first-principles derivation of SPH, but the key concepts and equations are recapped here.

SPH starts with the density estimate. This is a foundational quantity, and is used in almost every subsequent equation. It is calculated at any given point as the sum over all particles, which provide a contribution weighted by their distance:

$$\rho(\vec{r}_i) = \sum_j m_j W(|\vec{r}_i - \vec{r}_j|, h). \tag{1}$$

Here, $\vec{r}_i$ is a position (typically, but not necessarily, that of a particle) and $\vec{r}_j$ is the position of particle j, and m_j the mass of particle j. $W(\vec{r})$ is a function known as the weighting function, and is a function of a distance (here the

particle separation) and a smoothing length h. The weighting function W is related to a kernel $w(q)$ by $W(|\vec{r_i} - \vec{r_j}|, h) = \frac{1}{h} w(|\vec{r_i} - \vec{r_j}|/h)$.

The kernel is an important part of SPH. Most codes use an approximation to the Gaussian function which is truncated at a certain multiple of h. The value at which the kernel is truncated is known as the 'compact support radius', and this truncation increases computational efficiency by ignoring the negligible influence of extremely distant particles. This code uses the Schoenberg M_5 quartic spline kernel:

$$w(q) = \frac{1}{24} \begin{cases} (\frac{5}{2} - q)^4 - 5(\frac{3}{2} - q)^4 + 10(\frac{1}{2} - q)^4, & 0 \leq q < 0.5 \\ (\frac{5}{2} - q)^4 - 5(\frac{3}{2} - q), & 0.5 \leq q < 1.5 \\ (\frac{5}{2} - q)^4, & 1.5 \leq q < 2.5 \\ 0. & q \geq 2.5 \end{cases} \tag{2}$$

Once a satisfactory density estimate is obtained using the weighting function as described above, it can be employed in equations of motion that are derived using Lagrangian mechanics. To summarize, it can be shown that the acceleration is given by:

$$\frac{d\vec{v}_i}{dt} = -\sum_j m_j \left(\frac{P_i}{\rho_i^2} + \frac{P_j}{\rho_j^2} \right) \nabla_i W_{ij}(h), \tag{3}$$

where $W_{ij}(h)$ is shorthand for $W(|\vec{r_i} - \vec{r_j}|, h)$. Here, P_i and P_j refer to pressures, which are given by an equation of state that varies depending on the test being conducted.

Note that this equation is modified to add artificial viscosity and account for variable smoothing lengths as follows:

$$\frac{d\vec{v}_i}{dt} = -\sum_j m_j \left[\frac{P_i}{\Omega_i \rho_i^2} \nabla_i W_{ij}(h_i) + \frac{P_j}{\Omega_j \rho_j^2} \nabla_i W_{ij}(h_j) + \Pi_{ij} \nabla_i W_{ij} \left(\frac{h_i + h_j}{2} \right) \right]. \tag{4}$$

Here, Ω_i is an expression defined by

$$\Omega_i \equiv 1 - \frac{\partial h_i}{\partial \rho_i} \sum_j m_j \frac{\partial W_{ij}(h_i)}{\partial h_i}, \tag{5}$$

and Π_{ij} is an artificial viscosity parameter, the definition of which is explained in Bate (1995).

1.2 Ghost particles

A slight problem with the above equations of motion is that if particles acquire acceleration due to being 'repelled' by their neighbours, particles near the boundary will experience a net acceleration away from the origin, and move off towards infinity. To prevent this, boundary conditions are needed.

The choice of boundary condition for this program was the use of ghost particles. These are particles which exist only to 'correct' the density estimate at the edges and are not evolved or simulated like the other particles. This program generates ghost particles by selecting all the particles within a distance of the boundary equal to $2.5h$, and mirroring them around the boundary. This generation process is repeated part-way through each time-step to ensure the boundary conditions remain appropriate as the simulation progresses.

For uniform distributions, this appears to do a good job of producing an isotropic density estimate on setup. Figure 1 is a position-density plot that shows separately the ghost particles and alive particles. Note that the density estimate is virtually constant within the (-1, 1) boundary – and how this contrasts to a density profile without ghost particles such as Figure 3 where there is a large drop in density within the bounds of the simulation.

1.3 Variable smoothing length

It is desirable to modify the smoothing length h on a per-particle basis, so that regions of higher density have a lower smoothing length (and thus higher resolution) and to keep the number of neighbours for each particle approximately constant. The relationship between smoothing length and density is

$$h = h_{\text{fact}} \left(\frac{m}{\rho} \right), \tag{6}$$

where h_{fact} is a parameter that can be used to control the approximate number of neighbours for each particle, with $N_{\text{neigh}} \approx 5h_{\text{fact}}$.

To enforce this relation and find h, the root of the following equation is found using Newton-Raphsen iteration:

$$f(h_i) = \rho_{\text{sum}}(h_i) - \rho(h_i) = 0, \tag{7}$$

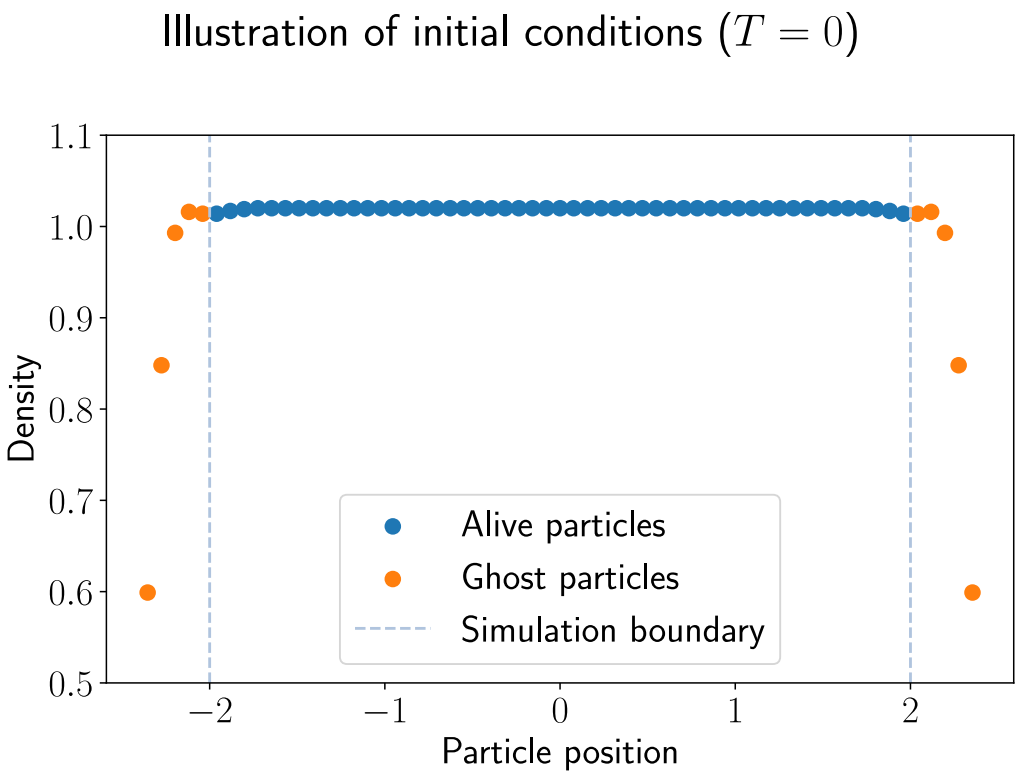

Figure 1: Plot showing density profile when 10 ghost particles are added to a simulation with 51 alive particles. This preserves a roughly constant initial density through (-1, 1) boundary of the simulation.

in which $\rho_{\text{sum}}(h_i)$ refers to the density as calculated by summation in Equation 1, and $\rho(h_i)$ refers to a rearranged form of the relation in Equation 6. Explicitly, this leads to the following equation and derivative:

$$f(h_i) = \sum_j m_j W_{ij}(h_i) - h_{\text{fact}} \left(\frac{m_i}{h_i} \right) = 0 \tag{8}$$

$$f'(h_i) = \sum_j m_j \frac{\partial W_{ij}(h_i)}{\partial h_i} + h_{\text{fact}} \left(\frac{m_i}{h_i^2} \right) = 0 \tag{9}$$

Figure 2 shows how smoothing length varies as a function of position for $T = 1$ of a colliding isothermal streams test (which is detailed in Section 2.3,

with a density plot given in Figure 5). Due to the high density peak in the centre of the distribution, smoothing length is minimized here and reduced towards the edges where there are fewer particles.

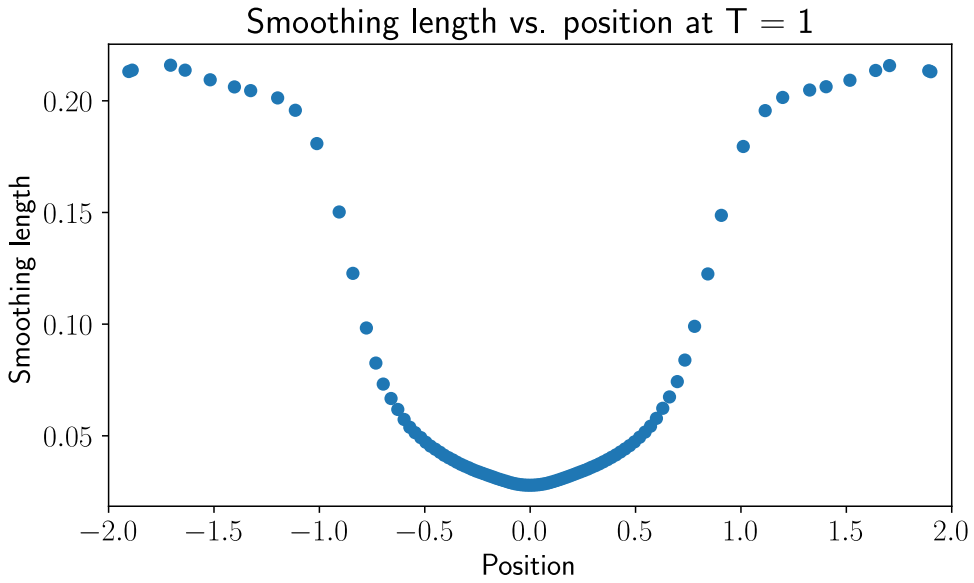

Figure 2: Plot showing the variation of smoothing length with position for T = 1 during the isothermal colliding streams test (Section 2.3, Figure 5). There is a high density region in the centre, where particles are given lower smoothing lengths, and the particles in the lower-density region are given high smoothing lengths.

1.4 Integration

The program makes use of a velocity Verlet integrator. It employs a time-step that is configurable in an external text file, but that is constant across all particles and across the duration of the simulation.

2 Results

2.1 Behaviour of density estimate along the axis

For this test, a random distribution of particles with $m = 1$ are used to test the effect of smoothing length on the density profile of the system. The variable smoothing length, as described in Section 1.3 is disabled for this test. Figure 3 is a plot showing different $\rho(\vec{r}, h)$ vs. x curves at different values of h. It shows that small values of h are very sensitive to the random nature of the distribution of particles, whilst large values of h effectively cancel out the random nature of the distribution and produce a smooth curve with a lower average density.

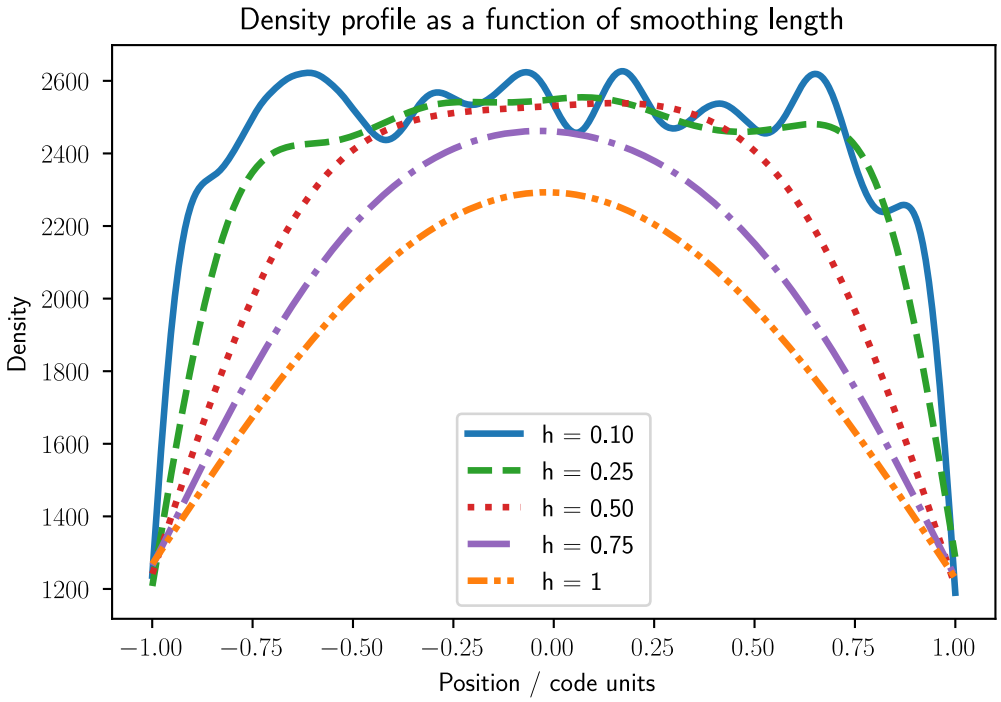

Figure 3: Plot showing density profiles at various values of h, for a random distribution of 1000 particles. Note that for $h = 1$, the compact support radius of the kernel at any given particle includes every single other particle in the distribution.

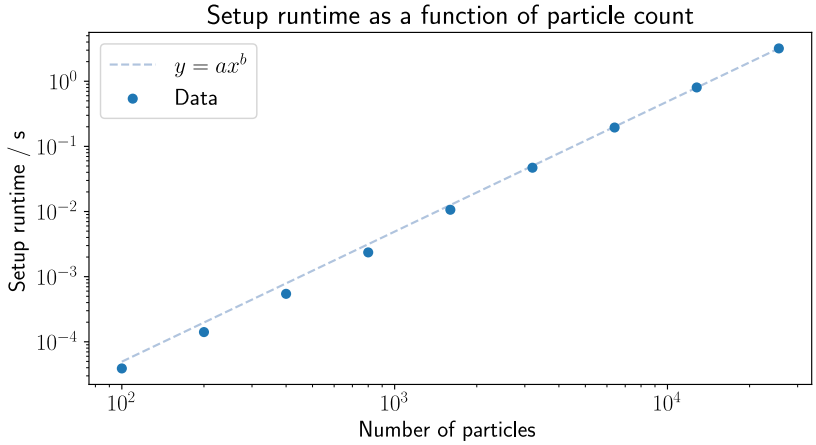

Figure 4: Log-log plot showing setup runtime as a function of particle count, ranging from 100 to 25,600. A constant $h = 0.2$ was used. A fit against $y = ax^b$ is performed establish the parameters of the exponential scaling relation, and it obtains $a = 5.021 \times 10^{-9}$ and $b = 1.997$.

2.2 Relation between setup runtime and number of particles

This test, like the above, features a random distribution of particles and a constant smoothing length. The aim is to investigate how the setup runtime (i.e. the time taken for the program to initialize the array of particles and calculate the density for each of them) varies with the number of particles requested. Figure 4 is a plot showing the results of this test. The fit against $y = ax^b$ obtains $a = 5.021 \times 10^{-9}$ and $b = 1.997$. This roughly aligns with the expectation of $O(N^2)$ scaling.

2.3 Isothermal colliding streams test

This test, outlined in Bate (1995), aims to reproduce an analytical result from a simulation. It makes use of variable smoothing lengths. 101 particles are distributed uniformly along an axis which ranges between $(-2, 2)$. They are then given a velocity

$$v_0 = \begin{cases} +c_s & x < 0, \\ -c_s & x \geq 0. \end{cases} \tag{10}$$

where $c_s = 1$ is an isothermal sound speed. This produces two colliding streams of particles, which meet at the origin. The equation of state used to determine pressure is

$$P = c_s^2 \rho. \tag{11}$$

The initial conditions are that $\rho_0 = 1$ and $c_s = 1$, which corresponds the following analytical solution at simulation time $T = 1$:

$$v = \frac{-v_0 + \sqrt{v_0^2 + 4}}{2}, \tag{12}$$

$$\frac{\rho_1}{\rho_0} = \frac{P_1}{P_0} = 1 + \frac{v_0}{v}. \tag{13}$$

Here ρ_1 and P_1 respectively refer to the density and pressure within the shocked region. v refers to the velocity of the outgoing shockwaves.

Figure 5 show graphical results from this test, which are compared with a similar figure from Bate (1995). Dashed lines corresponding to the numerical analytical solution are also shown. Partial reproduction is achieved, with the density of the shocked region being very close to the result predicted by Equation 13. However, the velocity of the outgoing shockwave is difficult to measure as it varies by position – though the result seem to be broadly similar to the predictions.

2.4 Adiabatic colliding streams test

This test also features two colliding streams, but there are several key differences. First, a different equation of state is used, where

$$P = (\gamma - 1) u \rho, \tag{14}$$

in which γ is a polytropic index (set to 5/3), and u is an internal energy, which is evolved on a per-particle basis, with

$$\frac{du_i}{dt} = \frac{P_i}{\Omega_i \rho_i^2} \sum_j m_j \vec{v}_{ij} \cdot \nabla_i W_{ij}(h_{ij}) + \frac{1}{2} \sum_j m_j \Pi_{ij} \vec{v}_{ij} \cdot \nabla_i W_{ij}(h_{ij}), \tag{15}$$

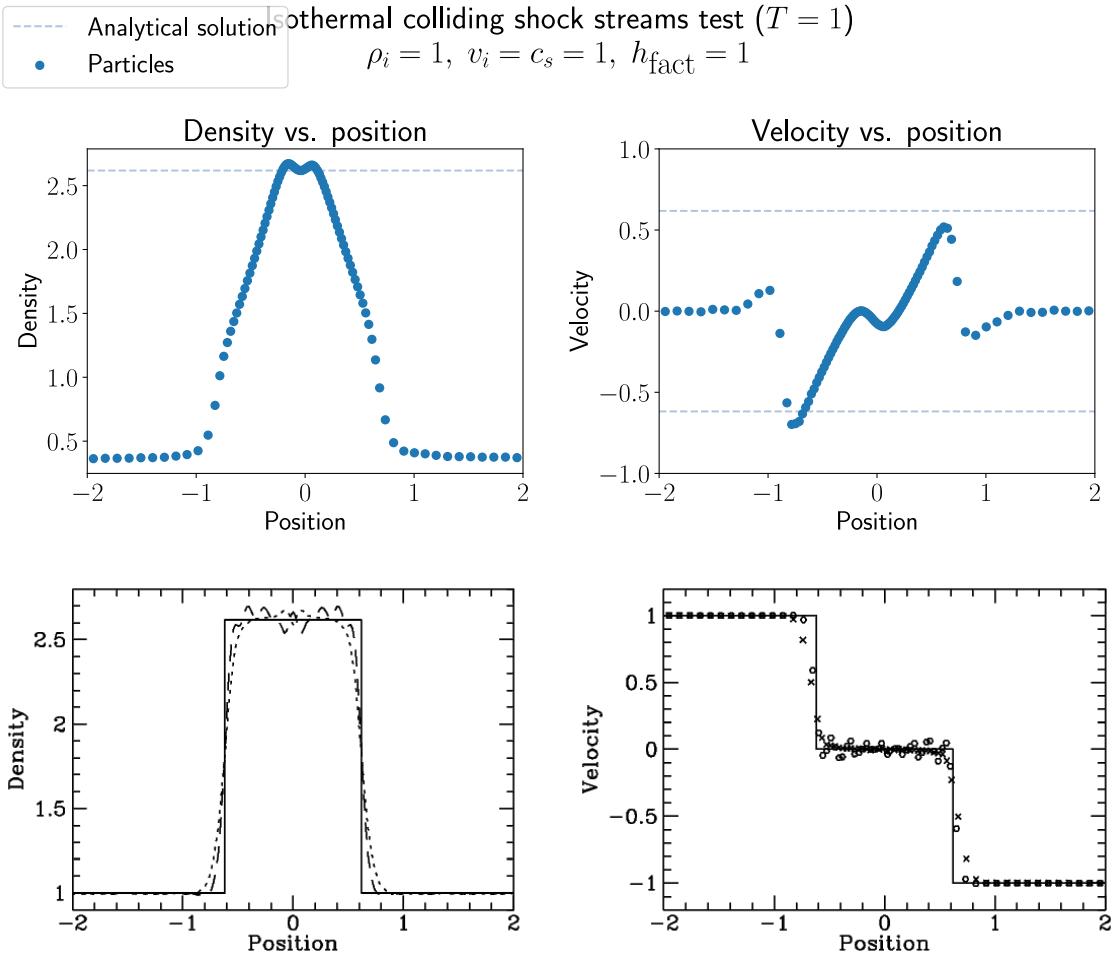

Figure 5: Comparison of this code's density profile result for the isothermal colliding streams test (upper) with that of Bate (1995) (lower). 101 particles and $h_{\rm fact} = 1$ are used for this test. The dashed lines in the top figure correspond to the analytical solutions described by Equations 12 and 13.

where $h_{ij} = \frac{h_i + h_j}{2}$. In addition, while the initial velocities are still set according to the sound speed as in Equation 10, in this case the sound speed is now given by $c_s = \sqrt{\gamma P/\rho}$ (simplifying to $c_s = \sqrt{\gamma}$ for $T = 0$). Finally, the initial internal energy u_0 is set to $1/(\gamma - 1)$. This test also has an analytical solution, defined by the following relations:

$$v = \frac{(\gamma - 3)v_0 + \sqrt{(\gamma + 1)^2 v_0^2 + 16\gamma}}{4}, \tag{16}$$

$$\frac{\rho_1}{\rho_0} = 1 + \frac{v_0}{v}, \tag{17}$$

$$\frac{u_1}{u_0} = \frac{\rho_0}{\rho_1} + v_0 v, \tag{18}$$

$$\frac{P_1}{P_0} = 1 + v_0(v + v_0). \tag{19}$$

Figure 6 shows the plotted output of the adiabatic simulation, which again compared against the analytical results and a figure from Bate (1995). The curves are smoother than expected and only vaguely resemble step functions. Moreover, the values for density and pressure in the shocked regions are too low. That said, they do reproduce a few of the same non-analytical quirks from Bate (1995), such as spikes around the centre of the distribution.

References

Price, Daniel J (2012). "Smoothed particle hydrodynamics and magnetohydrodynamics". In: *Journal of Computational Physics* 231.3, pp. 759–794.

Bate, Matthew Russell (1995). "The Role of Accretion in Binary Star Formation". PhD thesis. University of Cambridge.

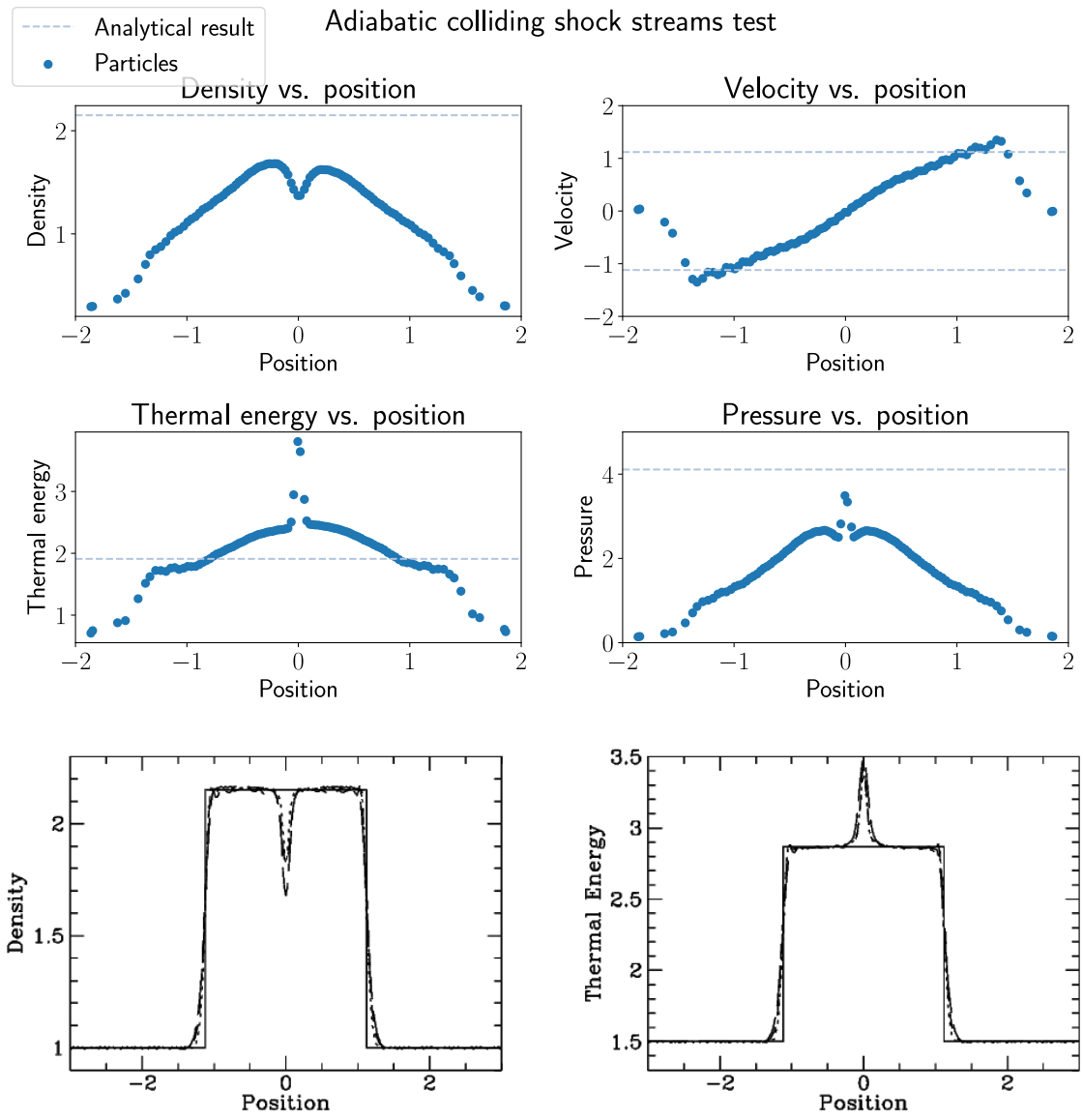

Figure 6: Comparison of this code's density profile result for the adiabatic colliding streams test (upper) with that of Bate (1995) (lower). This test used 101 particles and $h_{\text{fact}} = 2$. Analytical solutions from Equations 16 to 19 are included as dashed lines.